Utilization of realistic nano-scale voxel model of DNA matter for estimating DNA damage due to charged particle exposure

Jae-Hun Ryu and Eun-Hee Kim*
Department of. Nuclear Engineering, Seoul National University,
1 Gwanak-ro, Gwanak-gu, Seoul 08826, Republic of Korea
**Corresponding author: eunhee@snu.ac.kr*

1. Introduction

The key event of radiation in bio-organism is destruction of DNA structure. DNA consists of deoxyribose, phosphate, and nucleobases. Phosphate and deoxyribose molecules make up the backbone of DNA helix. As radiation passes through this structure, a strand of helix can be destroyed and this is called strand break (SB). When both strands of DNA helix within 10 base pairs (bps) are broken, they are viewed as a double strand break (DSB). SBs are readily repaired, whereas DSBs are less capable of repair, developing into cell destruction or mutation. [1] Hence, the number of DSBs induced from radiation exposure better indicates the possible cellular damage.

The DSB production is observed most commonly via γ-H2AX assay, in which the number of fluorescent antibodies attached to the DSB-induced protein is counted. [2] However, the number of DSBs observed by this method does not exactly match the number of DSBs that actually occurred because of DSB recovery by time and statistical variation in biological response.[3] Computational simulation can be employed to estimate DNA damage based on data libraries of physical, physicochemical, and chemical processes of radiation in biomatter. Geant4-DNA, an extension of Geant4, enables tracking radiation down to nano-scale. [4-5]

In a previous study, Abu Shqair et al. calculated the DSB production using the volume ratio of DNA matter to cell nucleus while simulating the probable radiation hit of DNA matter. [6] In this study, a geometrical model of chromatin fiber of an actual nm-scale was used to simulate radiation hits of DNA matter. The radiation events are recorded in terms of energy deposition and SB production yields per track. In addition, we validate the energy threshold for DNA SB by comparing SB production yields at varying cut-off energies for SB production.

2. Methods

2.1 DNA geometry model

The DNA structure shown in Fig. 1 was composed using DNA fabric software written in c++. The DNA structure consists of a combination of nucleotide pairs, which are the basic units of DNA. The nucleotide pair consists of phosphate groups, 2-deoxyribose, and nucleobases (adenine, guanine, cytosine and thymine) as presented in Fig. 2. [7] The water volume surrounding the nucleotide pairs was designated as the area from which the radical products can be transmitted to the nucleotide pairs. [8] Several nucleotide pairs surrounding a histone form a nucleosome. The rest form a linker between nucleosomes. The DNA geometry used in this study has a total 3,640 bps including 18 nucleosomes and 19 linkers. It is positioned inside a cube with a side length of 40 nm.

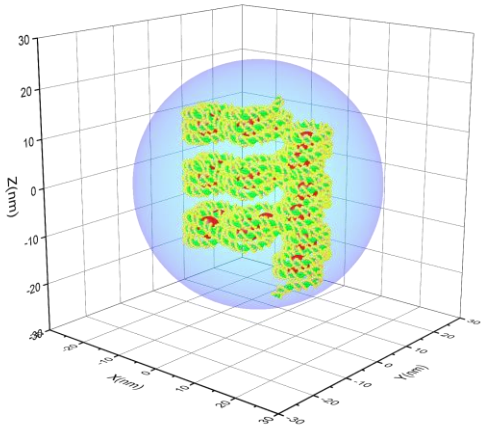

Figure 1. A DNA structure model used in simulation. DNA matter is positioned in a cube of 40 nm × 40 nm × 40 nm. Green components are nucleobases and yellow components are the backbone of DNA helix. Red components are histones. Incident particles start from random positions on the surface of blue sphere.

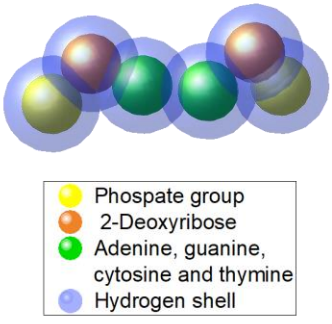

Figure 2. Schematic representation of a nucleotide pair model. [7] The nucleotide pair is surrounded by a hydration shell.

2.2 Simulation of physical interactions

Geant4-DNA (version 10.07) simulates the interactions of the incident particle and secondary electrons with DNA structure. [9-12] Whenever an interaction occurs, the location is specified among histone, deoxyribose, phosphate, adenine, guanine, thymine, cytosine, and the hydrogen shell. The location and deposited energy are recorded. Liquid water fills the DNA structure, approximating the biological medium. Default physics constructor "G4EmDNAPhysics" is used to employ the Geant4-DNA extension.

2.3 Determination of SBs

SB is induced when an energy over a threshold is deposited in the DNA backbone components, phosphate and deoxyribose. The energy of 17.5 eV has been a conventional choice for the threshold. [13] Energy deposition in the hydration shell surrounding a nucleotide pair may also cause SBs via producing reactive species. Since the threshold energy is still under discussion, we performed simulations applying the additional thresholds ranging from 12.5 eV to 30 eV. The SB production due to energy deposition over the threshold was compared with the previous estimate where the SB production was determined by random sampling based on the probabilities of SB induction for individual energy depositions. The probability increases linearly from 0 to 1 while energy deposition varies from 5 eV to 37.5 eV. [14]

2.4 Settings of simulation

The DNA structure of 40 nm × 40 nm × 40 nm is exposed to charged particles that are incident in an arbitrary direction from an arbitrary location on the spherical surface of 25 nm in radius. The spherical surface co-entered with the DNA structure. The primary particles are mono-energetic protons and alpha particles of 0.1 MeV, 0.5 MeV, 1 MeV, 2 MeV, 3 MeV, 4 MeV, 5 MeV, 7.5 MeV and 10 MeV. The simulation for each primary particle was performed 1,000 times at individual initial energies.

3. Results

3.1 Average energy deposition and average SB

Figs. 3 and 4 present the average energy depositions in the DNA structure and the average number of SBs, respectively, caused by alpha particles and protons that recorded any hit. Fig. 3 informs that an alpha particle delivers more energy to the DNA structure than a proton carrying the same initial energy as alpha particle. Both alpha particle and proton deposit more energy when they carry lower energy. Protons are expected to show the highest energy deposition when carrying energy less than 0.5 MeV. The energy deposition along the track in the DNA structure cannot represent the conventional LET (linear energy transfer) given by energy per μm because the track length is at most $40\sqrt{3}$ nm. In Fig. 4, the number of SBs varies consistently with the energy deposition. Table 1 summarizes the percentage of the simulation histories of alpha particle and proton that record no hit on the DNA structure and no SB production out of 1000 simulations. With higher conventional LET, alpha particles resulted in lower percentages of no hit and no SB production than protons.

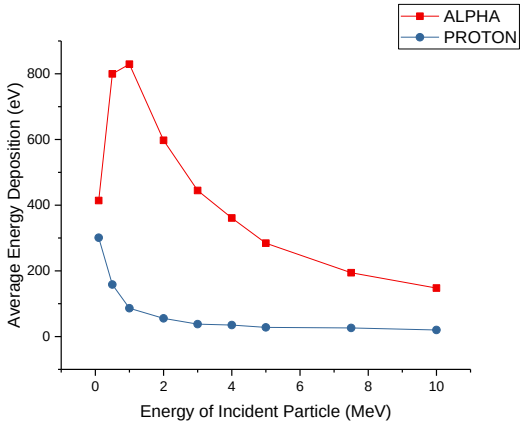

Figure 3. Average energy deposition per incident particle of energies up to 10 MeV that results in any hit on the DNA structure.

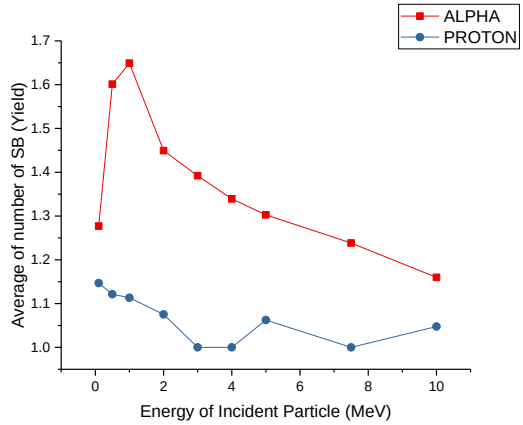

Figure 4. The yields of SBs per incident particle of energies up to 10 MeV that results in any hit on the DNA structure, assuming 17.5 eV as a threshold for SB induction.

Table 1. Percentages of no SB induction and no energy deposition for alpha particles and protons.

Incident energy (MeV)	no SB with alpha	no energy deposition with alpha	no SB with proton	no energy deposition with proton
0.1	76.9	0.2	82.3	0
0.5	56.4	0.4	86	0.4
1	50.8	0.6	90.3	2.7
2	56.6	0	94.7	6.8
3	60.2	0	96.7	14
4	66.4	0	97.2	20.6
5	71.6	0	98.4	23.7
7.5	76.1	0.3	97.8	34.2
10	83.1	0.4	97.9	43.9

3.2 Effect of the threshold energy for SB induction

More SBs are induced when the threshold energy for SB production is lower, which is demonstrated in Figs. 5 and 6. It is noticeable that SB yield maintains regardless of the threshold energy above 17.5 eV, which implies that the majority of discrete energy depositions along the track of alpha particles and protons is below 17.5 eV. Since the SB yield increases when the threshold is set at 12.5 eV instead of 17.5 eV, quite a portion of discrete energy depositions belong to the range from 12.5 eV to 17.5 eV. The SB yields assuming the linearly increasing probability of SB induction with the energy deposition are lower than those assuming the threshold of 12.5 eV, which implies that the SB yield attributing to the energy depositions of less than 12.5 eV is minimal.

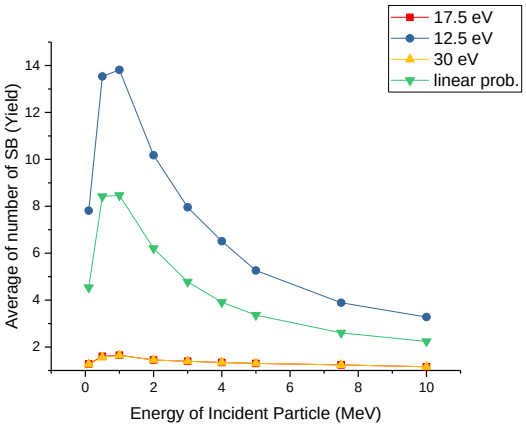

Figure 5. Average number of SBs per incident alpha particle of energies up to 10 MeV that resulted in any hit on the DNA structure. SBs were counted assuming different threshold energies for SB, 17.5 eV (red square), 12.5 eV (blue circle), 30 eV (yellow triangle), and compared with the counts obtained for the probability of SB induction linearly increasing with deposited energy (green triangle).

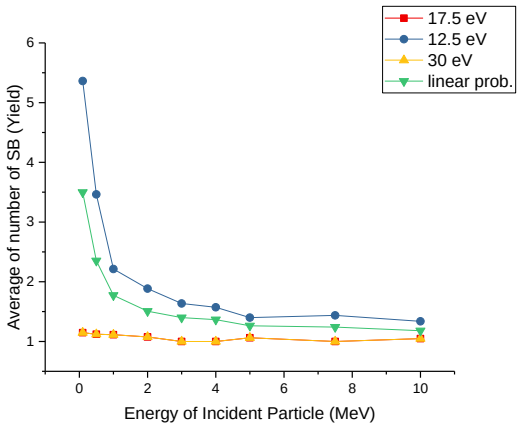

Figure 6. Average number of SBs per incident proton of energies up to 10 MeV that resulted in any hit on the DNA structure. SBs were counted assuming different threshold energies for SB, 17.5 eV (red square), 12.5 eV (blue circle), 30 eV (yellow triangle), and compared with the counts obtained for the probability of SB induction linearly increasing with deposited energy (green triangle)

3.3 Distribution of SB yields

Figs. 7 and 8 present the distribution of SB yields per incident alpha particle and proton, respectively. As summarized in Table 1, greater portions of incident protons resulted in no SB induction as compared to the incident alpha particles. Alpha particles of 1 MeV in incident energy recorded the peak energy deposition and the peak SB yield (Figs. 3 and 4), which is consistent with the largest SB yield in Fig. 7. Since the incident proton energy resulting in the peak energy deposition and the highest SB yield is presumed to be less than 100 keV (Figs. 3 and 4), the highest SB yield per incident proton is recorded at the least energy of 100 keV as shown in Fig. 8.

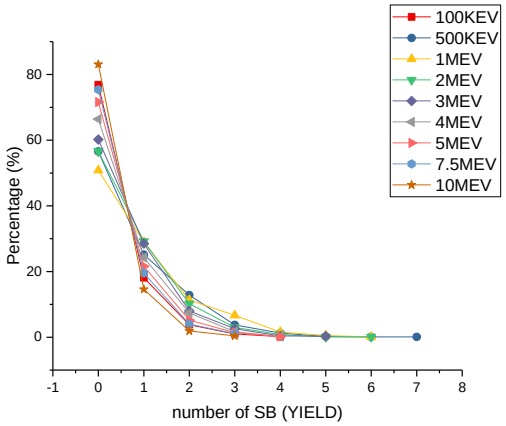

Figure 7. Distributions of SB yield per incident alpha particle from tracking 1000 alpha particles at each energy.

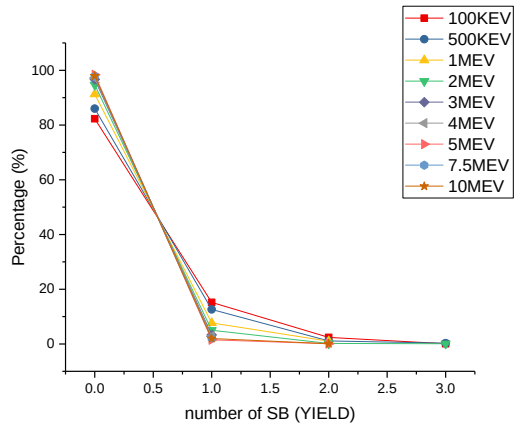

Figure 8. Distributions of SB yield per incident proton from tracking 1000 protons at each energy.

4. Conclusion

In this Study, the transport of alpha particle and proton were simulated by employing the realistic DNA structure model in nm-scale formulated by DNA Fabric Software. More realistic estimates of the yield of DNA strand breaks by charged particles were available due to energy deposition histories in a nanometer-scaled target volume.

REFERENCES

[1] B. K. Singleton, C. S. Griffin and J. Thacker, Clustered DNA Damage Leads to Complex Genetic Changes in Irradiated Human Cells, Cancer Research 62, 6263-6269, 2002.
[2] L. J. Mah, A. El-Osta and TC. Karagiannis, gammaH2AX: A Sensitive Molecular Marker of DNA Damage and Repair, Leukemia 24, 679-686, 2010.
[3] M. Lobrich et al., Gamma-H2AX Foci Analysis for Monitoring DNA Double-strand Break Repair: Strengths, Limitations and Optimization, Cell Cycle, 9:4, 662-669, 2010.
[4] S. Agostinelli et al., GEANT4-a Simulation Toolkit, Nuclear Instruments and Methods in Physics Research A 506, 250-303, 2003.
[5] M. Karamitros et al., Modeling Radiation Chemistry in the Geant4 Toolkit, Progress in Nuclear Science and Technology, Vol 2, 503-508, 2011.
[6] Ali Abu Shqair and Eun-Hee Kim, Multi-scaled Monte Carlo Calculation for Radon-induced Cellular Damage in the Bronchial Airway Epithelium, Sci. Rep. 11:10230, 2021.
[7] S. Meylan et al., Geant4-DNA Simulations Using Complex DNA Geometries Generated by the DnaFabric tool, Computer Physics Communications 204, 159-169, 2016.
[8] S. G. Swarts et al., Radiation-induced DNA Damage as a Function of Hydration, Radiation Research 129, 333-344, 1992.
[9] S. Incerti et al., Geant4-DNA Example Applications for Track Structure Simulations in Liquid Water: a Report from the Geant4-DNA Project, Med. Phys. 45, 722-739, 2018.
[10] M. A. Bernal et al., Track Structure Modeling in Liquid Water: A Review of the Geant4-DNA Very Low Energy Extension of the Geant4 Monte Carlo Simulation Toolkit, Phys. Med. 31, 861-874, 2015.
[11] S. Incerti et al., Comparison of Geant4 Very Low Energy Cross Section Models with Experimental Data in Water, Med. Phys. 37, 4692-4708, 2010.
[12] S. Incerti et al., The Geant4-DNA project, Int. J. Model. Simul. Sci. Comput. 1, 157-178, 2010.
[13] H. Nikjoo, P. O'Neill, W. E. Wilson and D. T. Goodhead, Computational Approach for Determining the Spectrum of DNA Damage Induced by Ionizing Radiation, Radiation Research 156, 577-583, 2001.
[14] W. Friedland et al., Simulation of DNA Damage after Proton Irradiation, Radiation Research 159, 401-410, 2003.